INTERNATIONAL JOURNAL FOR NUMERICAL METHODS IN FLUIDS, VOL. 24, 423–439 (1997)

A WAVE EQUATION MODEL TO SOLVE THE MULTIDIMENSIONAL TRANSPORT EQUATION

JIANKANG WU

Mechanics Department, Huazhong University of Science and Technology, Wuhan, Hubei 430074, People's Republic of China

SUMMARY

The wave equation model, originally developed to solve the advection–diffusion equation, is extended to the multidimensional transport equation in which the advection velocities vary in space and time. The size of the advection term with respect to the diffusion term is arbitrary. An operator-splitting method is adopted to solve the transport equation. The advection and diffusion equations are solved separately at each time step. During the advection phase the advection equation is solved using the wave equation model. Consistency of the first-order advection equation and the second-order wave equation is established. A finite element method with mass lumping is employed to calculate the three-dimensional advection of both a Gaussian cylinder and sphere in both translational and rotational flow fields. The numerical solutions are accurate in comparison with the exact solutions. The numerical results indicate that (i) the wave equation model introduces minimal numerical oscillation, (ii) mass lumping reduces the computational costs and does not significantly degrade the numerical solutions and (iii) the solution accuracy is relatively independent of the Courant number provided that a stability constraint is satisfied.

KEY WORDS: transport equation; wave equation model; FEM; mass lumping

1. INTRODUCTION

The transport equation arises naturally in several areas of environmental science and energy engineering. In many cases advection plays a dominant role in transport process. The numerical solution of the advection-dominated transport equation has been one of the most difficult problems in computational fluid dynamics. It is known that the advection component is the main source of difficulties in solving the transport equation. Many numerical papers have been published over the past decade. An accurate and effective numerical method for solving the transport equation is of great interest. In physics the advection equation represents the conservation laws of fluid mechanics. The mass, energy and momentum carried by fluid particles remain conservative in a flow field. The general solution of the advection equation is similar to a progressive wave in the flow direction where physical information is transferred from upstream to downstream and the advection equation is non-symmetric. Symmetric numerical methods such as central finite differences and the Galerkin finite element method are not likely to solve the advection equation accurately. It is preferable to adopt a numerical method consistent with the physical nature of the problem being considered. The characteristic method[1] and upwind method[2] are typical non-symmetric numerical methods which have been widely used. The characteristic method with linear interpolation gives a smooth but seriously damped solution. The characteristic method with high-order interpolation, developed by

CCC 0271–2091/97/050423–17

Received 21 December 1994
Revised 12 June 1996

Holly and Preissmann,[1] greatly reduces the numerical diffusion in one- or two-dimensional problems. In three dimensions the characteristic method with high-order interpolation is much more complex than in two dimensions. The upwind finite element method with asymmetric weighting functions improves the numerical solutions of the advection equation, but the first-order upwind model may introduce serious numerical diffusion.[3] Furthermore, the upwind parameter depends on both the magnitude and direction of the local advection velocities. It is very difficult to find a proper upwind parameter in cases where the advection velocities are non-uniform and unsteady. The second-order wave equation is symmetric or nearly symmetric and its solutions involve progressive waves in both directions of the flow. It may be expected that the wave equation can be solved accurately by symmetric numerical methods such as the well-known Galerkin finite element method. Consistency of the first-order advection equation and the second-order wave equation is established in this paper. The main idea behind a wave equation model is to solve a wave equation to obtain the solution of the advection equation. In particular, the discretized wave equation has better numerical properties than the discretized advection equation. The numerical solutions of the wave equation model display little oscillation. The wave equation model introduces both numerical diffusion and inverse numerical diffusion[4] because it involves advection in both flow directions; thus the final numerical diffusion error is small.

Mass lumping diagonalizes the coefficient matrix and reduces the memory requirement. Moreover, a linear system solver is not required and thus the computational costs are significantly reduced. Equivalence of the wave and advection equations is demonstrated and consistency is established in Section 2. A finite element method for the wave equation model (WEM/FEM) and a solution procedure for the wave equation model of the transport equation are described in Section 3. Numerical examples of advection in 3D of both a Gaussian cylinder and sphere in translational and rotational flow fields are given in Section 4. Advection-dominated transport of a cloud parcel is presented as the final example.

2. EQUIVALENCE OF THE WAVE EQUATION TO THE ADVECTION EQUATION

In an operator-splitting method the transport equation is split into advection and diffusion components. The advection equation is written as

$$\frac{\partial C}{\partial t} + \vec{V} \cdot \nabla C = 0 \tag{1}$$

where the advection velocity $\vec{V}$ is a known function of time and space. The initial condition is given as

$$C(x, y, z, t_0) = C_0(x, y, z). \tag{2}$$

Boundary conditions on the inflow boundaries are specified as

$$C(x, y, z, t) = C_{\text{in}}(x, y, z, t) \quad \text{on} \quad \partial\Omega_{\text{in}}. \tag{3}$$

A boundary condition is not needed on the outflow boundary for the advection equation (1). It is difficult to solve the advection equation directly, especially in a multidimensional space where the advection velocities are non-uniform and unsteady. The numerical dispersion and numerical diffusion

soon render unphysical solutions. To avoid these difficulties, one may transform the first-order advection equation into a second-order wave equation by differentiating the advection equation (1). Positive and negative advection equations are defined as

$$\left(\frac{\partial}{\partial t}+\vec{V}\cdot\nabla\right)C=\left(\frac{\partial}{\partial t}+U\frac{\partial}{\partial s}\right)C=0, \tag{4}$$

$$\left(\frac{\partial}{\partial t}-\vec{V}\cdot\nabla\right)C=\left(\frac{\partial}{\partial t}-U\frac{\partial}{\partial s}\right)C=0, \tag{5}$$

where U is the magnitude of the advection velocity and $\vec{s}$ is the unit vector of the local flow direction. The solutions of equations (4) and (5) represent positive advection and negative advection in the flow direction respectively. The advection equation (4) is differentiated by the negative advection operator as

$$\left(\frac{\partial}{\partial t}-\vec{V}\cdot\nabla\right)\left(\frac{\partial}{\partial t}+\vec{V}\cdot\nabla\right)C=0. \tag{6}$$

Expanding equation (6) yields a wave equation

$$\frac{\partial^2 C}{\partial t^2}=\vec{V}\vec{V}::\nabla\nabla C+\left(-\frac{\partial\vec{V}}{\partial t}+(\vec{V}\cdot\nabla)\,\vec{V}\right)\cdot\nabla C, \tag{7}$$

where the first term on the right is a double inner product of second-order tensors. A detailed derivation of equation (7) is given in the Appendix. Equation (6) can also be written as

$$\left(\frac{\partial}{\partial t}-U\frac{\partial}{\partial s}\right)\left(\frac{\partial}{\partial t}+U\frac{\partial}{\partial s}\right)=0 \quad \text{in flow co-ordinates.} \tag{8}$$

Expanding equation (8) yields a wave equation

$$\frac{\partial^2 C}{\partial t^2}=U^2\frac{\partial^2 C}{\partial s^2}+\left(-\frac{\partial U}{\partial t}+U\frac{\partial U}{\partial s}\right)\frac{\partial C}{\partial s} \quad \text{in flow co-ordinates.} \tag{9}$$

The wave equations (7) and (9) are identical. Physically, equation (9) implies that the wave equation involves positive advection and negative advection in the flow direction. If the advection velocity is constant, the wave equation (9) is reduced to the classical wave equation

$$\frac{\partial^2 C}{\partial t^2}=U^2\frac{\partial^2 C}{\partial s^2}. \tag{10}$$

The general solutions of equation (10) consist of progressive waves in both directions of the flow. The physical information involved in the wave equation (9) is transferred in both directions of the flow; the advection equation transfers the information in only one direction. It can be seen that the wave equation is symmetric or nearly symmetric; the advection equation is non-symmetric. For the wave equation an additional initial condition is given as

$$\frac{\partial C}{\partial t}=-\vec{V}\cdot\nabla C_0 \quad \text{at} \quad t=t_0, \tag{11}$$

where C_0 is given by equation (2). Both inflow and outflow boundary conditions are required for the wave equation (9). The inflow boundary condition is given in equation (3). The outflow boundary condition is obtained from the advection equation. In fact, the solution on the outflow boundary is part of the advection equation (1); it cannot be specified arbitrarily. In other words, the advection equation must be imposed on the outflow boundaries. The outflow boundary condition is written as

$$C(x, y, z, t) = C_{\text{out}}(x, y, z, t) \quad \text{on} \quad \partial\Omega_{\text{out}}. \tag{12}$$

We need to demonstrate that the solutions of the wave equation and advection equation are equivalent before numerical discretization. The advection equation may be written as

$$A = 0, \tag{13}$$

where $A = \partial C/\partial t + \vec{V} \cdot \nabla C$ is defined as the advection function. The wave equation is written as

$$\left(\frac{\partial}{\partial t} - \vec{V} \cdot \nabla\right) A = 0. \tag{14}$$

The advection function A is constant along characteristics:

$$\frac{\mathrm{d}x}{\mathrm{d}t} = -u, \qquad \frac{\mathrm{d}y}{\mathrm{d}t} = -v, \qquad \frac{\mathrm{d}z}{\mathrm{d}t} = -w, \tag{15}$$

where u, v and w are the three components of the advection velocity $\vec{V}$. A characteristic through a point (x, y, z, t) in the solution space can be tracked backwards in time to either the departure point of the initial space ($t = t_0$) or the outflow boundary. If the two conditions

$$A = 0 \quad \text{at} \quad t = t_0 \quad \text{everywhere} \tag{16}$$

and

$$A = 0 \quad \text{on the outflow boundary} \quad \text{for} \quad t \geq t_0 \tag{17}$$

are imposed, then $A = 0$ (i.e. the advection equation is satisfied) can be guaranteed everywhere inside the solution space (x, y, z, t). Conditions (16) and (17) are the same as equations (11) and (12). Therefore the solution of the wave equation is the same as the solution of the advection equation after imposing conditions (16) and (17). In fact, the physical information on the outflow boundaries comes from inside the domain. Condition (17) requires that the first-order advection equation be imposed on the outflow boundaries to obtain the solutions on the outflow boundaries. The characteristic method is one of the most effective methods for solving the advection equation and is used to calculate the outflow boundary solutions in this paper.

3. WEM/FEM FORMULATION OF THE TRANSPORT EQUATION

A finite element method (WEM/FEM) for the solution of the wave equation model of the transport equation is presented in this section. A general transport equation can be written as

$$\frac{\partial C}{\partial t} + \vec{V} \cdot \nabla C = D\nabla^2 C + aC + Q, \tag{18}$$

where D is a diffusion coefficient, a is a first-order chemical reaction coefficient and Q is a source term. In an operator- splitting method the transport equation is split into an advection equation and a diffusion equation:

$$\frac{\partial C}{\partial t} + \vec{V} \cdot \nabla C = 0, \tag{19}$$

$$\frac{\partial C}{\partial t} = D\nabla^2 C + aC + Q. \tag{20}$$

In physics the diffusion, chemical reaction and source terms are all local phenomena, so they appear in the diffusion equation (20). The advection equation (19) is solved using the wave equation model. For a finite element formulation an alternative form of the wave equation (7) can be written as

$$\frac{\partial^2 C}{\partial t^2} = \nabla \cdot [\vec{V}(\vec{V} \cdot \nabla C)] - \left(\frac{\partial \vec{V}}{\partial t} + \vec{V}(\nabla \cdot \vec{V})\right) \cdot \nabla C. \tag{21}$$

If the fluid is incompressible, equation (21) reduced to

$$\frac{\partial^2 C}{\partial t^2} = \nabla \cdot [\vec{V}(\vec{V} \cdot \nabla C)] - \frac{\partial \vec{V}}{\partial t} \cdot \nabla C. \tag{22}$$

A derivation of equation (21) can be found in the Appendix. A finite element formulation of the wave equation (22) is presented in Reference 4. A Galerkin formulation is applied to the wave equation (22), where integration by parts has been employed to obtain a weak form:

$$\left\langle \frac{\partial^2 C}{\partial t^2}, \varphi_i \right\rangle = \int_{\partial\Omega} (\vec{V} \cdot \nabla C) V_{\mathrm{n}} \varphi_i \mathrm{d}s - \langle (\vec{V} \cdot \nabla C), (\vec{V} \cdot \nabla \varphi_i) \rangle - \left\langle \left(\frac{\partial \vec{V}}{\partial t} \cdot \nabla C \right), \varphi_i \right\rangle, \tag{23}$$

where

$$\langle f, g \rangle = \int\int\int_{\Omega} f \cdot g \mathrm{d}x\mathrm{d}y\mathrm{d}z. \tag{24}$$

The inner product notation $\langle ., . \rangle$ denotes integration over the entire 3D domain. The ϕ_i ($i = 1, 2, \ldots$) are global interpolation functions. The boundary integral on the right-hand side of equation (23) disappears on boundaries with zero normal flux. At the nodes of inflow and outflow boundaries, equation (23) is replaced by essential boundary conditions. An inflow boundary condition is specified and the outflow boundary condition is calculated by the characteristic method from previous solutions inside the domain. At the internal nodes the boundary integral disappears and equation (23) is reduced to

$$\left\langle \frac{\partial^2 C}{\partial t^2}, \varphi_i \right\rangle = -\langle (\vec{V} \cdot \nabla C), (\vec{V} \cdot \nabla \varphi_i) \rangle - \left\langle \left(\frac{\partial \vec{V}}{\partial t} \cdot \nabla C \right), \varphi_i \right\rangle. \tag{25}$$

The time derivative term is approximated by finite differences; the other terms are weighted over three time levels $n+1$, n and $n-1$. The corresponding system equation of the wave equation (25) is written as

$$[A]\{C^{n+1}\} = [B]\{C^n\} + [E]\{C^{n-1}\}, \tag{26}$$

where the matrix coefficients are given by

$$A_{ij} = \int_\Omega \phi_j \phi_i \mathrm{d}\Omega + \theta \Delta t^2 \int_\Omega \left\{ (\vec{V} \cdot \nabla \phi_j)(\vec{V} \cdot \nabla \phi_i) + \frac{\partial \vec{V}}{\partial t} \phi_i \nabla \phi_j \right\}^{n+1} \mathrm{d}\Omega, \tag{27}$$

$$B_{ij} = 2 \int_\Omega \phi_j \phi_i \mathrm{d}\Omega - (1 - 2\theta) \Delta t^2 \int_\Omega \left\{ (\vec{V} \cdot \nabla \phi_j)(\vec{V} \cdot \nabla \phi_i) + \frac{\partial \vec{V}}{\partial t} \phi_i \nabla \phi_j \right\}^{n} \mathrm{d}\Omega, \tag{28}$$

$$E_{ij} = - \int_\Omega \phi_j \phi_i \mathrm{d}\Omega - \theta \Delta t^2 \int_\Omega \left\{ (\vec{V} \cdot \nabla \phi_j)(\vec{V} \cdot \nabla \phi_i) + \frac{\partial \vec{V}}{\partial t} \phi_i \nabla \phi_j \right\}^{n-1} \mathrm{d}\Omega. \tag{29}$$

Here the superscripts $n+1$, n and $n-1$ indicate that these terms are calculated at time levels $n+1$, n and $n-1$ respectively. Ω is the integral domain and θ is the time weighting factor ($0 \leqslant \theta \leqslant 0{\cdot}5$). If $\theta = 0$, i.e. an explicit scheme, then the matrices $[A]$ and $[E]$ contain only the first term, i.e.

$$A_{ij} = -E_{ij} = \int_\Omega \phi_j \phi_i \mathrm{d}\Omega. \tag{30}$$

These matrices can be mass lumped by summing all elements in a row and placing the results on the diagonal. A matrix solver is not needed. The counterpart of the matrix $[B]$ is also diagonalized. For the present problems the mass lumping significantly reduces the computational costs. Matrices involving space derivatives cannot be diagonalized. Mass lumping has been used by many researchers.[5] It can be seen in the numerical examples that mass lumping does not degrade the numerical solutions. Several different numerical methods could be used to solve the wave equation (7). A finite element method with mass lumping has proven to be an effective technique. The objective of this paper is to demonstrate that the wave equation model is one of the most accurate and effective numerical methods for solving the transport equation. The diffusion equation (20) is solved by a finite element method and a Crank– Nicolson time-stepping scheme where a natural boundary condition has been imposed. The essential boundary condition needs to be specified. The finite element formulation of the diffusion equation is well established. The details will not be presented here. The finite element system of the diffusion equation is written as

$$[H]\{C^{n+1}\} = [P]\{C^n\} + \{f\}, \tag{31}$$

where the matrix coefficients are given by

$$H_{ij} = \left(1 - \frac{a\Delta t}{2}\right) \int_\Omega \phi_j \phi_i \mathrm{d}\Omega + \frac{D\Delta t}{2} \int_\Omega \nabla \phi_j \nabla \phi_i \mathrm{d}\Omega, \tag{32}$$

$$P_{ij} = \left(1 + \frac{a\Delta t}{2}\right) \int_\Omega \phi_j \phi_i \mathrm{d}\Omega - \frac{D\Delta t}{2} \int_\Omega \nabla \phi_j \nabla \phi_i \mathrm{d}\Omega, \tag{33}$$

$$\{f\} = \int_\Omega Q^{n+1/2} \phi_i \mathrm{d}\Omega. \tag{34}$$

Here the source term is evaluated at time level $n + \frac{1}{2}$. The solution algorithm for solving the transport equation using a wave equation model is shown in Figure 1, where the horizontal direction denotes the diffusion process and the vertical direction denotes the advection process. C_0^{n-1} and C_0^{n+1} are the intermediate solutions at time levels $n-1$ and $n+1$ respectively. The wave equation model is a three-time-level algorithm. The new solution C^{n+1} is computed using the old solutions C^{n-1} and C^n.

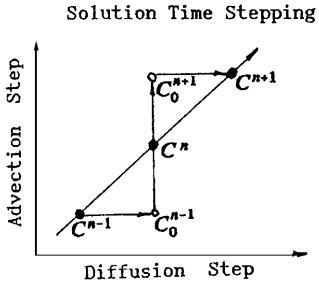

Figure 1. Sketch of solution procedure for WEM/FEM

Substep 1. Solve the diffusion equation $C^{n-1} \xrightarrow{FEM} C_0^{n-1}$, i.e.

$$[H]\{C_0^{n-1}\} = [P]\{C^{n-1}\} + \{f^{n-1/2}\}, \tag{35}$$

where

$$f_i^{n-1/2} = \int_\Omega Q^{n-1/2}\phi_i \mathrm{d}\Omega. \tag{36}$$

Substep 2. Solve the wave equation C_0^{n-1}, $C^n \xrightarrow{FEM} C_0^{n+1}$, i.e.

$$[A]\{C_0^{n+1}\} = [B]\{C^n\} + [E]\{C_0^{n-1}\}. \tag{37}$$

Substep 3. Solve the diffusion equation $C_0^{n+1} \xrightarrow{FEM} C^{n+1}$, i.e.

$$[H]\{C^{n+1}\} = [P]\{C_0^{n+1}\} + \{f^{n+1/2}\}. \tag{38}$$

4. ERROR ANALYSIS OF THE WAVE EQUATION MODEL IN TWO DIMENSIONS

We now present a truncation error analysis of WEM/FEM for solving the advection equation in two-dimensional space. The following assumptions are made to simplify the analysis.

1. The advection velocities are uniform in space and steady in time.
2. The space grids are uniform.
3. The second-order time derivative is approximated by central finite differences.
4. The space derivatives are approximated by a Galerkin finite element method and evaluated at time level n (explicit scheme).
5. The coefficient matrix is diagonalized by mass lumping.

Assuming $\Delta x = \Delta y$ and $u = v$, the wave equation (7) is reduced to

$$\ddot{C} = u^2 C_{2s} + 2uvC_{xy} + v^2 C_{2y}, \tag{39}$$

$$\ddot{C} = U^2 C_{2s} \quad \text{in flow co-ordinates}, \tag{40}$$

where the superscript double dot denotes a second-order time derivative and the subscripts denote space derivatives. For example, C_{2x} is the second-order derivative with respect to x. One internal node is connected with eight neighbouring nodes, as shown in Figure 2. Node 5 is the internal node.

The finite element equation of node 5 contains nine terms in two dimensions. The finite element equation for node 5 can be written as

$$\sum_{j=1}^{9} a_j \ddot{C}_j = \frac{u^2}{\Delta x^2} \sum_{j=1}^{9} b_j C_j, \tag{41}$$

where the coefficients a_j and b_j are calculated by a Galerkin finite element method. The wave equation and node structure are symmetric, as are the coefficients, i.e.

$$a_1 = a_9, \qquad a_2 = a_8, \qquad a_3 = a_7, \qquad a_4 = a_6, \tag{42}$$
$$b_1 = b_9, \qquad b_2 = b_8, \qquad b_3 = b_7, \qquad b_4 = b_6. \tag{43}$$

Symmetric nodes such as nodes (1, 9), (2, 8), etc. have the same contribution to the finite element equation at internal node 5. The coefficients are found to be

$$a_1 = \tfrac{1}{36}, \qquad a_2 = \tfrac{1}{9}, \qquad a_3 = \tfrac{1}{36}, \qquad a_4 = \tfrac{1}{9}, \qquad a_5 = \tfrac{1}{4}, \tag{44}$$
$$b_1 = \tfrac{5}{6}, \qquad b_2 = \tfrac{1}{3}, \qquad b_3 = \tfrac{1}{6}, \qquad b_4 = \tfrac{1}{3}, \qquad b_5 = -\tfrac{3}{8}. \tag{45}$$

Equation (41) is expanded as a Taylor series at node 5. Each term of equation (41) is expanded as

$$C_j = C_5 + \sum_{n=1}^{\infty} (\Delta x_j C_x + \Delta y_j C_y)^n, \quad j = 1, 2, \ldots, 9, \tag{46}$$

$$\ddot{C}_j = \ddot{C}_5 + \sum_{n=1}^{\infty} (\Delta x_j \ddot{C}_x + \Delta y_j \ddot{C}_y)^n, \quad j = 1, 2, \ldots, 9. \tag{47}$$

Owing to the node symmetry, it follows that

$$\Delta x_1 = -\Delta x_9, \qquad \Delta y_1 = -\Delta y_9, \qquad \Delta x_2 = -\Delta x_8, \qquad \Delta y_2 = \Delta y_8 = 0,$$
$$\Delta x_3 = -\Delta x_7, \qquad \Delta y_3 = -\Delta y_7, \qquad \Delta x_4 = \Delta x_6 = 0, \qquad \Delta y_4 = -\Delta y_6.$$

The terms on the left side of equation (41) are written as

$$a_1(\ddot{C}_1 + \ddot{C}_9) = 2a_1 \left(\ddot{C}_5 + \sum_{n=2,4,\ldots}^{\infty} \frac{1}{n!} (\Delta x \ddot{C}_x + \Delta y \ddot{C}_y)^n \right), \tag{48}$$

$$a_2(\ddot{C}_2 + \ddot{C}_8) = 2a_2 \left(\ddot{C}_5 + \sum_{n=2,4,\ldots}^{\infty} \frac{1}{n!} (\Delta x \ddot{C}_x)^n \right), \tag{49}$$

$$a_3(\ddot{C}_3 + \ddot{C}_7) = 2a_3 \left(\ddot{C}_5 + \sum_{n=2,4,\ldots}^{\infty} \frac{1}{n!} (\Delta x \ddot{C}_x - \Delta y \ddot{C}_y)^n \right), \tag{50}$$

$$a_4(\ddot{C}_4 + \ddot{C}_6) = 2a_4 \left(\ddot{C}_5 + \sum_{n=2,4,\ldots}^{\infty} \frac{1}{n!} (\Delta y \ddot{C}_y)^n \right). \tag{51}$$

By adding equations (48)–(51), the left side of equation (41) can be written as

$$\mathrm{LS} = \ddot{C}_5 + \tfrac{1}{6}\Delta x^2 C_{2x} + \tfrac{1}{6}\Delta y^2 \ddot{C}_{2y} + \tfrac{1}{72}\Delta x^4 \ddot{C}_{4x} + \tfrac{1}{72}\Delta y^4 \ddot{C}_{4y} + \tfrac{1}{36}\Delta x^2 \Delta y^2 \ddot{C}_{2x,2y} + \mathrm{HOT}. \tag{52}$$

The left side of equation (41) is the second-order time derivative of equation (52), which should not be related to the neighbouring nodes. Except for the first term, all the other terms may be considered as error caused by the finite element approximation. If mass lumping is used, i.e. adding all the coefficients a_j to term 5, one finds

$$\sum_{j=1}^{9} a_j = 1. \tag{53}$$

Finally, the left side of equation (41) becomes

$$\mathrm{LS} = \ddot{C}_5. \tag{54}$$

Equation (54) is exactly the same as before the finite element method was applied. Following the above procedure, the right side of equation (41) can be written as

$$\begin{aligned}\mathrm{RS} = \frac{u^2}{\Delta x^2}[&\Delta x^2 C_{2x} + 2\Delta x\Delta y C_{x,y} + \Delta y^2 C_{2y} + \tfrac{1}{12}(\Delta x^4 C_{4x} + \Delta y^4 C_{4y} \\ &+ 4\Delta x\Delta y^3 C_{x,3y} + 4\Delta x^3\Delta y C_{3x,y} + 4\Delta x^2\Delta y^2 C_{2x,2y})] + \mathrm{HOT}.\end{aligned} \tag{55}$$

By co-ordinate transformation, equation (55) can be written in flow co- ordinates as

$$\ddot{C} = U^2 C_{2s} + \tfrac{1}{12}\Delta s^2 U^2[C_{4s} - \tfrac{1}{8}(C_{2s} - C_{2n})^2] + \mathrm{HOT}. \tag{56}$$

where s is flow direction, n is normal to flow direction in two-dimensions. The second time derivative of equation (56) is approximated by finite differences as

$$\ddot{C} = \frac{C^{n+1} - 2C^n + C^{n-1}}{\Delta t^2}. \tag{57}$$

Substituting equation (57) into equation (56) yields

$$\ddot{C} = U^2 C_{2s} + \tfrac{1}{12}\Delta s^2 U^2[(1 - C_r^2)C_{4s} - \tfrac{1}{8}(C_{2s} - C_{2n})^2] + \mathrm{HOT}, \tag{58}$$

where the Courant number is defined as

$$Cr = \frac{u\Delta t}{\Delta x}. \tag{59}$$

The leading term of the truncation error is the fourth-order space derivative. It may be expected that the numerical solutions of the wave equation will exhibit little oscillation. The error analysis in three-dimensional space can be carried out in the same way but is more difficult. Given the same assumptions, a similar result can be expected.

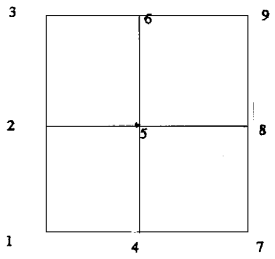

Figure 2. Local discretized grids for truncated error analysis for WEM/FEM

5. NUMERICAL EXAMPLES

It is difficult to find a three-dimensional numerical example of the advection in a non-uniform and unsteady flow field. Park and Ligget[6] provides a three-dimensional example employing the Taylor least squares finite element method. In this work the advection velocity is non-uniform but steady. A number of three-dimensional examples of advection with WEM/FEM are given in this section. The advection velocities are non-uniform and unsteady. In three dimensions a Gaussian cylinder is defined as

$$C(x, y, z) = \exp(-pr^2), \qquad r^2 = (x - x_0)^2 + (y - y_0)^2, \tag{60}$$

where p is a positive real number and (x_0, y_0) is the centre of the Gaussian cylinder. The Gaussian cylinder is uniform in z. When the distribution function C decreases to a small number, say 0·000001, r is defined as the radius of the Gaussian cylinder. Outside the cylinder the distribution function may be considered as zero. Similarly, a three-dimensional Gaussian sphere is defined as

$$C(x, y, z) = \exp(-pr^2), \qquad r^2 = (x - x_0)^2 + (y - y_0)^2 + (z - z_0)^2, \tag{61}$$

where (x_0, y_0, z_0) is the centre of the Gaussian sphere. The radius is defined in the same way as for the Gaussian cylinder. The eight-node isoparametric cube element and Lagrangian interpolation function are used. The time derivative is approximated by finite differences, the spatial derivative terms are calculated at time level n and the time weighting factor θ in equations (27)–(29) is zero. The coefficient matrices $[A]$ and $[E]$ of equation (26) are mass lumped.

Example 1 Advection of a three-dimensional Gaussian cylinder in a uniformly rotational flow field.

The centre of rotation coincides with the centre of the cylinder. The domain is a hexahedron of size 100 m × 100 m × 4 m. The advection velocity is designed to make the cylinder rotate uniformly about its axis. The flow velocity is as given as

$$u = -\omega(y - y_0), \qquad v = \omega(x - x_0), \tag{62}$$

where ω is the angular rotation rate. The centre of the cylinder is located at $x_0 = y_0 = 50$ m. The domain is discretized into 5000 subcubes of size 2 m × 2 m × 2 m. The radius of the cylinder is about 40 m and the solutions on the inflow boundaries are set to zero. The solutions on the outflow boundaries are calculated with characteristics. The numerical solutions after one and two revolutions are shown in Figures 3(a) and 3(b) respectively. The numerical solutions are accurate compared with the exact solutions. The solution shape is well maintained. The peak values of the Gaussian cylinder have been reduced to 99·6 per cent and 94·5 per cent respectively.

Example 2 Advection of a three-dimensional Gaussian cylinder in a periodically rotational flow field.

The centre of rotation coincides with the centre of the cylinder. The domain size and other parameters are the same as in Example 1. In the flow field the cylinder rotates about its axis periodically. The flow velocity is specified as

$$\omega(t) = \sin(\bar{\omega}t), \qquad u = -\omega(t)(y - y_0), \qquad v = \omega(t)(x - x_0), \tag{63}$$

where the cylinder rotates a half-revolution (π) in the first half- period, then rotates back to the original position in the second half-period. The numerical solutions after one and two periods are shown in Figures 4(a) and 4(b) respectively. The peaks have been reduced to 99·2 per cent and 94·0 per cent respectively.

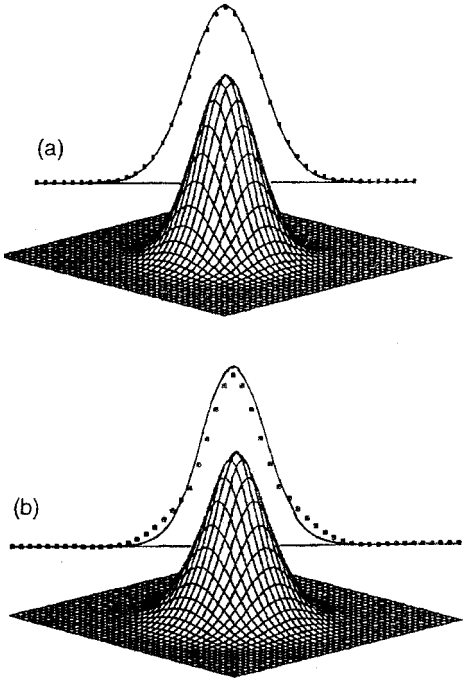

Figure 3. Numerical solutions for advection of Gaussian cylinder in uniformly rotational flow field when centre of cylinder coincides with centre of rotation: (a) after one revolution; (b) after two revutions: —— exact solution; ..... numerical solution

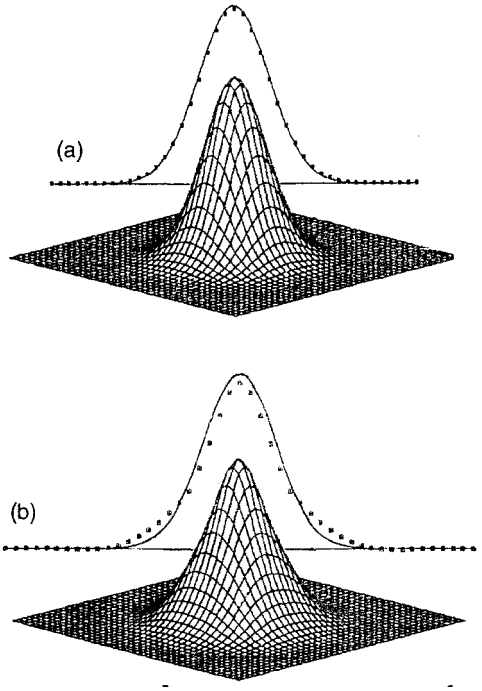

Figure 4. Numerical solutions for advection of Gaussian cylinder in periodically rotational flow field when centre of cylinder coincides with centre of rotation: (a) after one period; (b) after two periods: —— exact solution; ..... numerical solution

Example 3 Advection of a three-dimensional Gaussian cylinder in a uniformly rotational flow field.

The centre of rotation *does not* coincide with the centre of the cylinder. The advection velocity is the same as in equation (62). The domain size is 100 m × 100 m × 2·5 m, discretized into 12,800 subcubes of size 1·25 m × 1·25 m × 1·25 m. The centre of the Gaussian cylinder is located at $x_0 = 30$ m, $y_0 = 30$ m. The numerical solutions after a half- revolution and one revolution are shown in Figures 5(a) and 5(b) respectively. The peaks have been reduced to 99·2 per cent and 94·1 per cent respectively. The left hill in Figure 5(a) is the initial position of the Gaussian cylinder.

Example 4 Advection of a three-dimensional Gaussian cylinder in a periodically rotational flow field.

The centre of the cylinder *does not* coincide with the centre of rotation. The advection velocity is the same as in equation (63). The domain size and other parameters are the same as in Example 3. The Gaussian cylinder rotates about the centre of the domain periodically. The cylinder rotates back too the original position after one period. The numerical solutions after a half-period and one period are shown in Figures 6(a) and 6(b) respectively. The peaks have been reduced to 99·0 per cent and 92·8 per cent respectively. The left hill in Figure 6(a) is the initial position of the Gaussian cylinder.

Example 5 Advection of a three-dimensional Gaussian cylinder in a periodic flow field.

The domain size and other parameters are the same as in Example 3. In the flow field the cylinder moves in the diagonal of the domain periodically, as shown in Figure 7(a). The cylinder moves back to the original position after one period. The flow velocity is specified as

$$u = v = \sin(\omega t). \tag{64}$$

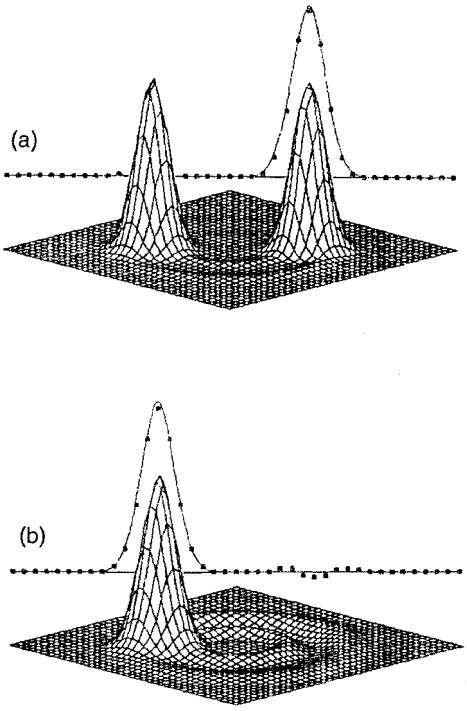

Figure 5. Numerical solutions of advection of Gaussian cylinder in uniformly rotational flow field when centre of cylinder does not coincide with centre of rotation: (a) after a half-revolution; (b) after one revolution: —— exact solution; . . . . . numerical solution

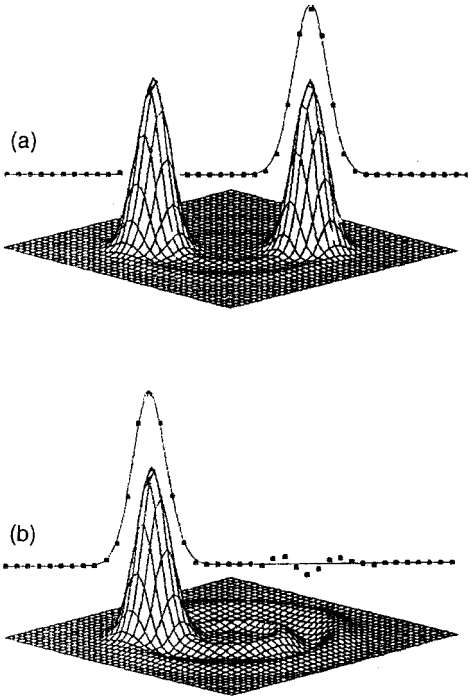

Figure 6. Numerical solutions of advection of Gaussian cylinder in periodically rotational flow field when centre of cylinder does not coincide with centre of rotation: (a) after a half-period; (b) after one period: ——— exact solution; . . . . . numerical solution

The initial centre of the cylinder is located at $x_0 = 20$ m, $y_0 = 20$ m. The numerical solutions after a half-period and one period are shown in Figures 7(b) and 7(c) respectively. The peaks have been reduced to 99·2 per cent and 99·0 per cent respectively. The left hill in Figure 7(b) is the initial position of the Gaussian cylinder.

Example 6 Advection of a three-dimensional Gaussian cylinder in a translational and rotational flow field.

The domain size and other parameters are the same as in Example 5. In the flow field the cylinder moves in the diagonal and rotates about its centre, as shown in Figure 8(a). The flow velocity is specified as

$$u(t) = u_0 - \omega(y - y_0 - u_0 t), \qquad v = v_0 + \omega(x - x_0 - v_0 t). \tag{65}$$

The cylinder moves 85 m in the diagonal and rotates about half- revolution (π). The numerical solution is shown in Figure 8(b). The peak has been reduced to 99·2 per cent. The left hill is the initial position of the Gaussian cylinder.

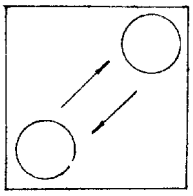

Figure 7(a). Sketch of advection of Gaussian cylinder in periodic flow field

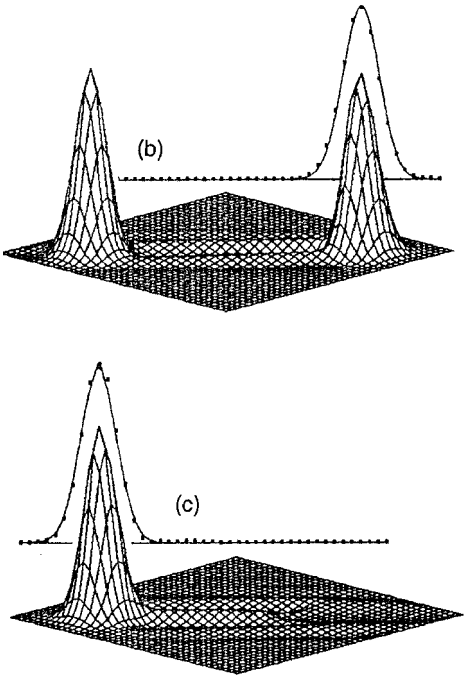

Figure 7(b, c). Numerical solutions of advection of Gaussian cylinder in periodic flow field: (b) after a half-period; (c) after one period: —— exact solution; . . . . . numerical solution

Example 7 Advection of a three-dimensional Gaussian sphere in a uniformly rotational flow field.

The domain size is 100 m × 100 m × 100 m, discretized into 125,000 subcubes of size 2 m × 2 m × 2 m. In the flow field the Gaussian sphere rotates about the diagonal of the cube domain, as shown in Figure 9(a). The flow velocity is specified as

$$u = \frac{\omega(z-y)}{\sqrt{3}}, \qquad v = \frac{\omega(x-z)}{\sqrt{3}}, \qquad w = \frac{\omega(y-x)}{\sqrt{3}}, \tag{66}$$

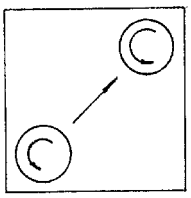

Figure 8(a). Sketch of advection of Gaussian cylinder in translational and rotational flow field

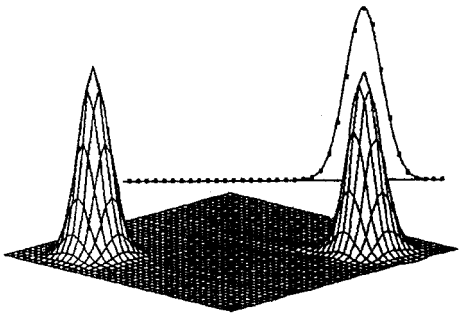

Figure 8(b). Numerical solution of advection of Gaussian cylinder in translational and rotational flow field: —— exact solution; . . . . . numerical solution

where ω is the rotation rate. The numerical solutions in an x–y plane through the sphere centre after one and two revolutions are shown in Figures 9(b) and 9(c) respectively. The peaks have been reduced to 99·5 per cent and 94·7 per cent respectively. The solution shape is well maintained.

Example 8 Advection of a three-dimensional Gaussian sphere in a periodically rotational flow field.

The domain size and other parameters are the same as in Example 7. The Gaussian sphere rotates about the diagonal of the domain periodically. The Gaussian sphere rotates back to the original position after one period. The numerical solutions after one and two periods are shown in Figures 10(a) and 10(b) respectively. The peaks have been reduced to 99·1 per cent and 93·1 per cent respectively.

Example 9 Advection-dominant transport of a two-dimensional cloud parcel in a uniform flow field.

The governing equation is written as

$$\frac{\partial C}{\partial t} + \vec{V} \cdot \nabla C = D\left(\frac{\partial^2 C}{\partial x^2} + \frac{\partial^2 C}{\partial y^2}\right). \tag{67}$$

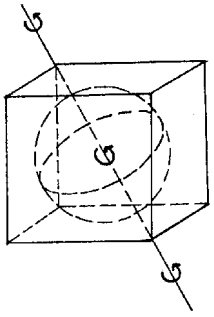

Figure 9(a). Sketch of advection of Gaussian sphere in rotational flow field

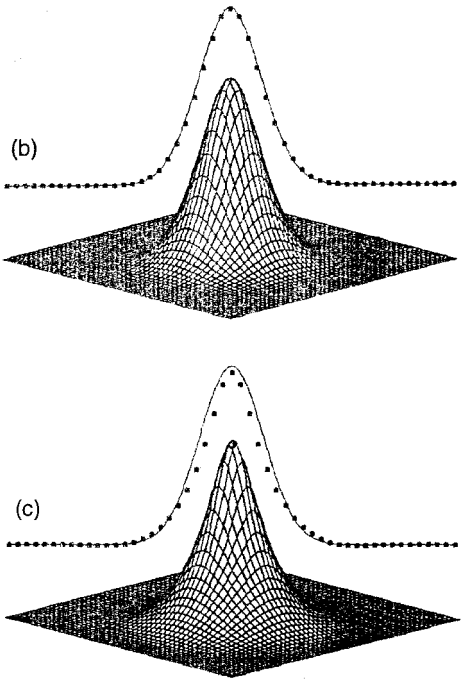

Figure 9(b, c). Numerical solutions of advection of Gaussian sphere in uniformly rotational flow field: (b) after one revolution; (c) after two revolutions: —— exact solution; . . . . . numerical solution

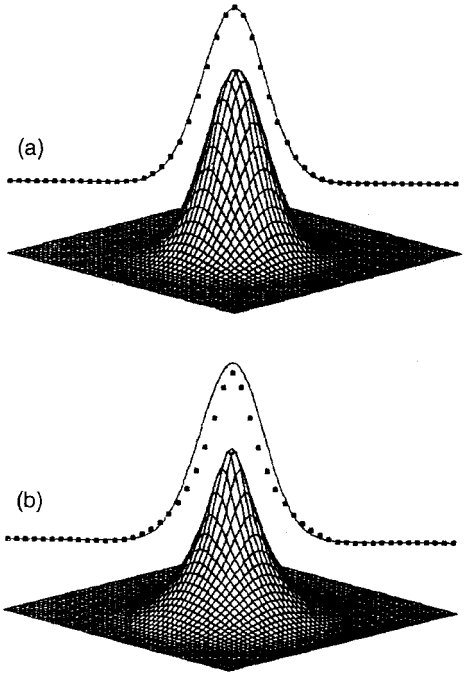

Figure 10. Numerical solutions of advection of Gaussian sphere in periodic rotational flow field: (a) after one period; (b) after two periods: —— exact solution; . . . . . numerical solution

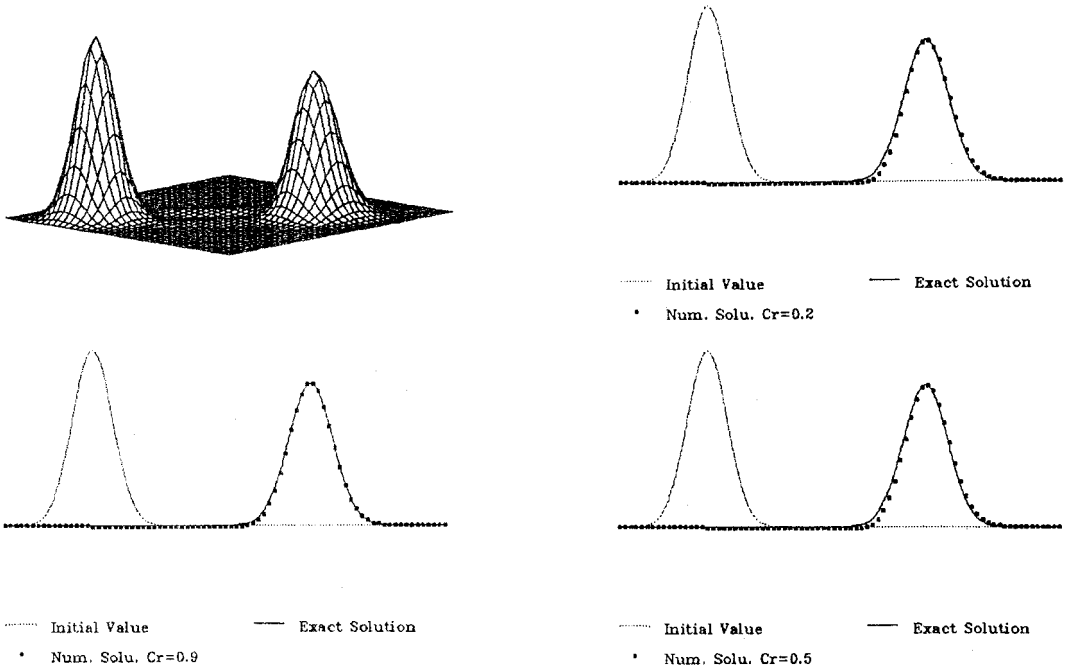

Figure 11. Numerical solutions of transport of cloud parcel for various Courant numbers

The solution domain size is 100 m × 100 m, discretized into 10,000 subsquares. The exact solution of the advection–diffusion of a cloud parcel is given as

$$C(x, y, t) = \frac{M}{4\pi Dt}\exp\left(-\frac{(x - x_0 - ut)^2 + (y - y_0 - vt)^2}{4Dt}\right), \tag{68}$$

where $M = 125$ m^2, $x_0 = 20$ m, $y_0 = 20$ m, $D = 0{\cdot}05$ m^2 s^{-1} and $u = v = 1$ m s^{-1}. The three-dimensional WEM/FEM code is used to test this problem. The solution of equation (68) at $t = 200$ s is taken as the initial value. The numerical solutions at $t = 250$ s are shown in Figure 11 for Courant numbers $Cr = 0{\cdot}9$, $0{\cdot}5$ and $0{\cdot}2$. The numerical solutions are accurate in comparison with the exact solutions.

6. DISCUSSION AND CONCLUSIONS

In this paper the two- and three-dimensional advection equation and advection- dominated transport equation were solved by WEM/FEM. The numerical results are fairly accurate compared with the exact solutions. The advection velocities are non-uniform and unsteady. The wave equation has good symmetry, but the first-order advection equation does not. Symmetrical numerical methods such as the Galerkin FEM can be used to solve the wave equation accurately. Mass lumping greatly reduces the computational costs and does not degrade the numerical solutions very much. For solving the wave equation, the finite element method with mass lumping adopted in this paper is one of the most effective numerical methods. If the system matrices are not mass lumped, the numerical solutions could be better than given in this paper. The objective of this paper is to demonstrate that the wave equation model is a good numerical model to solve a variety of advection-dominated transport problems. The wave equation model has the following notable properties.

1. It has the ability to eliminate numerical dispersion successfully. The numerical solutions exhibit little oscillation. The leading term of the truncation error is the fourth-order space derivative.
2. It introduces inverse numerical diffusion as well as numerical diffusion. They may be cancelled partly at least. The numerical solutions of the wave equation model are relatively independent of the Courant number under a stability constraint. The time step and space grid size may be flexible in the stability range.

The wave equation model is a relatively new numerical method for solving advection-dominated transport problems. Preliminary works have shown excellent numerical properties of WEM. Further study is needed in both theory and application, such as how the numerical diffusion and inverse numerical diffusion are created and how they are cancelled. More numerical experiments and verification in practical applications are also needed.

ACKNOWLEDGEMENTS

This research was supported by the National Science Foundation of China. The author would like to thank the referees for their instructive comments and kind help with the English.

APPENDIX

The left side of equation (6) is expanded as

$$\begin{aligned}
\mathrm{LS} &= \left(\frac{\partial}{\partial t} - \vec{V}\cdot\nabla\right)\left(\frac{\partial C}{\partial t} + \vec{V}\cdot\nabla C\right) \\
&= \frac{\partial^2 C}{\partial t^2} - \vec{V}\cdot\nabla\left(\frac{\partial C}{\partial t}\right) + \frac{\partial}{\partial t}(\vec{V}\cdot\nabla C) - \vec{V}\cdot\nabla(\vec{V}\cdot\nabla C) \\
&= \frac{\partial^2 C}{\partial t^2} - \vec{V}\cdot\nabla\left(\frac{\partial C}{\partial t}\right) + \vec{V}\cdot\frac{\partial}{\partial t}(\nabla C) + \frac{\partial \vec{V}}{\partial t}\cdot\nabla C - \vec{V}\cdot\nabla(\vec{V}\cdot\nabla C) \\
&= \frac{\partial^2 C}{\partial t^2} - \vec{V}\cdot\nabla\left(\frac{\partial C}{\partial t}\right) + \vec{V}\cdot\nabla\left(\frac{\partial C}{\partial t}\right) + \frac{\partial \vec{V}}{\partial t}\cdot\nabla C - \vec{V}\cdot\nabla(\vec{V}\cdot\nabla C) \qquad (69) \\
&= \frac{\partial^2 C}{\partial t^2} + \frac{\partial \vec{V}}{\partial t}\cdot\nabla C - \vec{V}\cdot\nabla(\vec{V}\cdot\nabla C) \\
&= \frac{\partial^2 C}{\partial t^2} + \frac{\partial \vec{V}}{\partial t}\cdot\nabla C - \vec{V}\vec{V}::\nabla\nabla C - (\vec{V}\cdot\nabla\vec{V})\cdot\nabla C \\
&= \frac{\partial^2 C}{\partial t^2} - \vec{V}\vec{V}::\nabla\nabla C + \left(\frac{\partial \vec{V}}{\partial t} - (\vec{V}\cdot\nabla)\vec{V}\right)\cdot\nabla C.
\end{aligned}$$

Finally, the wave equation is obtained as

$$\frac{\partial^2 C}{\partial t^2} = \vec{V}\vec{V}::\nabla\nabla C + \left(-\frac{\partial \vec{V}}{\partial t} + (\vec{V}\cdot\nabla)\vec{V}\right)\cdot\nabla C. \qquad (7)$$

Equation (69) can also be written as

$$\mathrm{LS} = \frac{\partial^2 C}{\partial t^2} + \frac{\partial \vec{V}}{\partial t}\cdot\nabla C - \nabla\cdot[\vec{V}(\vec{V}\cdot\nabla C)] + \vec{V}(\nabla\cdot\vec{V})\cdot\nabla C.$$

The wave equation can be expressed in an alternative form as

$$\frac{\partial^2 C}{\partial t^2} = \nabla\cdot[\vec{V}(\vec{V}\cdot\nabla V)] - \left(\frac{\partial \vec{V}}{\partial t} + \vec{V}(\nabla\cdot\vec{V})\right)\cdot\nabla C. \qquad (21)$$

Equation (21) is used in the finite element calculation.

REFERENCES

1. F. M. Holly Jr. and A. Preissmann, 'Accurate calculation of transport in two dimensions', *ASCE J. Hydraul. Div.*, **98**, 1259–1277 (1977).
2. O. C. Zienkiewicz and R. L. Taylor, *The Finite Element Method*, Vol. 2, McGraw-Hill, London, 1991.
3. C. A. J. Fletcher, *Computational Techniques for Fluid Dynamics*, Springer, Berlin, 1988.
4. J. K. Wu, 'Wave equation model for solving advection–diffusion equation', *Int. j. numer. methods eng.*, **37**, 2717–2733 (1994).
5. L. Lapidus and G. F. Pinder, *Numerical Solutions of Partial Differential Equations in Science and Engineering*, Wiley–Interscience, New York, 1982, pp. 567–571.
6. N. S. Park and J. A. Ligget, 'Application of Taylor-least square finite element to three-dimensional advection–diffusion equation', *Int. j. numer. methods fluids*, **13**, 759–773 (1991).